

Cite this: DOI: 10.1039/c2sc00770c

www.rsc.org/chemicalscience

EDGE ARTICLE

## Functionalizing molecular wires: a tunable class of $\alpha,\omega$ -diphenyl- $\mu,\nu$ -dicyano-oligoenes<sup>†‡</sup>

Jeffrey S. Meisner,<sup>a</sup> Danielle F. Sedbrook,<sup>a</sup> Markrete Krikorian,<sup>a</sup> Jun Chen,<sup>b</sup> Aaron Sattler,<sup>a</sup> Matthew E. Carnes,<sup>a</sup> Christopher B. Murray,<sup>bc</sup> Michael Steigerwald<sup>a</sup> and Colin Nuckolls<sup>\*a</sup>

Received 7th October 2011, Accepted 4th January 2012

DOI: 10.1039/c2sc00770c

We describe the synthesis and characterization of a new class of cyano-functionalized oligoenes and their derivatives. We have made the vinyllogous series of  $\alpha,\omega$ -diphenyl- $\mu,\nu$ -dicyano-oligoenes (DPDCn) comprised of each odd-numbered member from 3 to 13 linear conjugated olefins. Installing cyano groups onto the oligoene backbone lowers HOMO and LUMO energies by up to  $\sim 0.7$  eV, thereby stabilizing the molecule with respect to oxidative decomposition; this exemplifies a new approach to the stabilization of conjugated oligoenes. UV-vis absorption spectra and redox potentials across the DPDCn series reveal that the molecular band gap ranges from 2.80 to 1.75 eV. This gap can be further tuned by the facile installation of a variety of aryl end-groups. The choice of end-groups also greatly affects the physical properties such as solubility and the solid-state packing. We also present the longest oligoene crystal structure reported to date. Moreover, we find that the prototypical linear structure makes oligoenes suitable as molecular wires and connectors in the bottom-up construction of nanoscale architectures. As a proof of concept, carboxylic acid terminated oligoenes were used to position 10-nm Fe<sub>3</sub>O<sub>4</sub> nanoparticles on a GaAs (100) substrate.

### Introduction

In this study we present a new class of tunable, functional and easily derivatized molecular wires. These wires are noteworthy because they are molecularly defined, atomically precise fragments of polyacetylene (PA, Fig. 1a). PA is remarkable because it is a simple hydrocarbon polymer that is highly conductive when

doped.<sup>1</sup> It also has a low band gap and shows large nonlinear optical susceptibilities.<sup>2</sup> Since the fully conjugated high polymer of  $-\text{C}(\text{H})=\text{C}(\text{H})-$  is electrically conductive, we believe that well-defined oligomers, hereafter referred to as oligoenes, should be useful molecular conductors in nanoscale situations. In addition, naturally occurring terpenoid-based oligoenes, such as carotenoids, have been made into electrical devices and are known to have useful optical properties.<sup>3</sup> However, nature provides only a limited number of structures that are often difficult to functionalize further, thus preventing their use in widespread applications.

The synthesis and study of conjugated oligomers has bourgeoned over the past 20 years, however oligoene systems remain understudied. Three major challenges have hampered the development of oligoenes as electronic materials: (1) the most thoroughly studied examples of PA oligomers have been obtained inefficiently through the painstaking isolation of individual oligomers from polymerization reactions terminated at low monomer conversion.<sup>4</sup> (2) Previous preparative methods have not supported diverse functionalization to incorporate them into electronic devices. (3) Oligomers of PA are chemically impractical because they are nearly insoluble and oxidatively unstable. Using the new synthetic strategy detailed below for the  $\alpha,\omega$ -diphenyl- $\mu,\nu$ -dicyano-oligoenes<sup>5</sup> (DPDC, Fig. 1c) we have overcome these challenges. The key to this synthesis is the use of sterically innocent yet electronically stabilizing cyano groups bound directly to the oligoene chain while protecting the reactive

<sup>a</sup>Columbia University, Department of Chemistry, 3000 Broadway, Havemeyer Hall, New York, New York 10027, USA. E-mail: cn37@columbia.edu

<sup>b</sup>University of Pennsylvania, Department of Materials Science and Engineering, 3231 Walnut Street, Philadelphia, PA, 19104, USA

<sup>c</sup>Department of Chemistry, 231 S. 34th Street, Philadelphia, PA, 19104, USA

<sup>†</sup> Electronic supplementary information (ESI) available: List of all molecules, detailed synthetic procedures and characterization data of oligoenes, oligoene-aldehydes, Fe<sub>3</sub>O<sub>4</sub> nanoparticles, and nanoparticle-oligoene SAMs; UV-vis spectroscopic data; cyclic voltammetry; CIF files for DPDCn; DFT theoretical methods and results for DPDCn and DPOn and selected functionalized oligoenes. CCDC reference numbers 847946–847952. For ESI and crystallographic data in CIF or other electronic format see DOI: 10.1039/c2sc00770c

<sup>‡</sup> Funding sources: This material is based upon work supported by the National Science Foundation through the Centers for Chemical Innovation (CCI) under Grant No. CHE-0943957, Subaward No. UTA09-000882 as well as the Army Research Office (ARO) Multidisciplinary University Research Initiative (MURI) under award number W911NF-08-1-0364, subaward UCD 08-000678-CU-1. We thank the National Science Foundation under Grant No. CHE-0619638 for acquisition of an X-ray diffractometer.

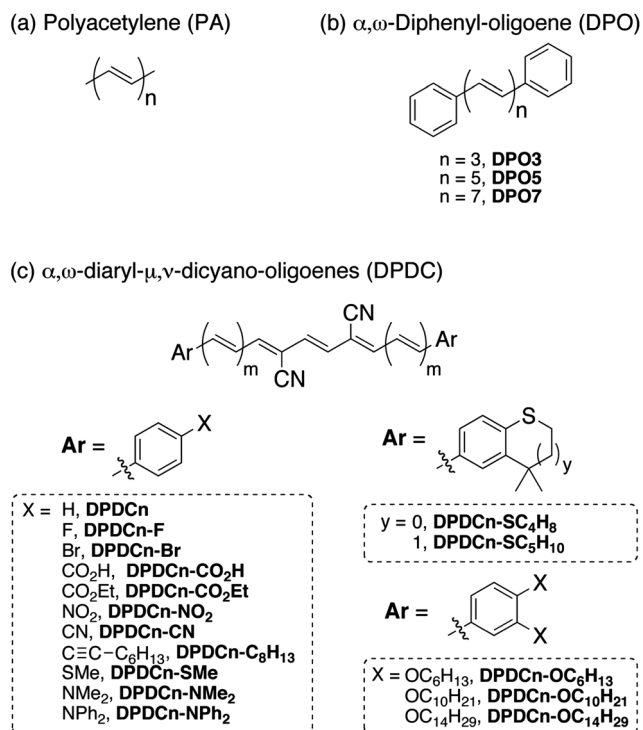


**Fig. 1** Structure of (a) polyacetylene (PA). (b) Structure of  $\alpha,\omega$ -diphenyl-oligoenes (DPO), which we regard as control molecules for comparison with (c) cyano-functionalized  $\alpha,\omega$ -diphenyl-oligoenes (DPDC). We identify the oligoene molecules according to the length of their linear conjugated backbone ( $n$ ) and aryl end-group ( $X$ ), **DPDCn-X**. For instance, 1,10-di(4-bromophenyl)-4,7-dicyano-deca-1,3,5,7,9-pentaene is denoted as **DPDC5-Br**. See ESI† for a complete list of molecules.

terminal olefins with bulky phenyl groups.<sup>6</sup> These phenyl end-groups can easily be modified with a diverse range of functionality. We recently reported<sup>7</sup> that alkylthio-terminated members of this family conduct electrically; here we extend that study to reveal the wide variety of compounds that can be produced through our synthetic method. We also highlight the versatility and adaptability of these new electronic materials by using appropriately functionalized oligoenes as electrical conduits that connect magnetic nanoparticles to a semiconductor surface.

Other methods have been used to stabilize oligoenes. Several approaches protect the highly reactive terminal olefins with bulky end-groups such as phenyl (DPO, Fig. 1b)<sup>6</sup> or *tert*-butyl.<sup>8,9</sup> Other than such hydrocarbon-end-capped oligoenes, however, there are few other examples of non-terpenoid  $\alpha,\omega$ -disubstituted oligoenes longer than pentaenes.<sup>10,11</sup> Nature provides its own methods of oligoene stabilization: carotenoids are the most well-studied oligoenes since they play essential roles in vision (retinal), cell differentiation (retinol) and photosynthesis.<sup>12</sup> In these molecules, methyl groups decorate the oligoene backbone and contribute to both the solubility and stability. However, they also create allylic strain along the poly-olefin backbone, which causes the molecules to bend. These distortions reduce the conjugation and increase the energy difference between the highest occupied molecular orbital (HOMO) and lowest unoccupied molecular orbital (LUMO), therefore shifting the electronic absorptions to higher energies.

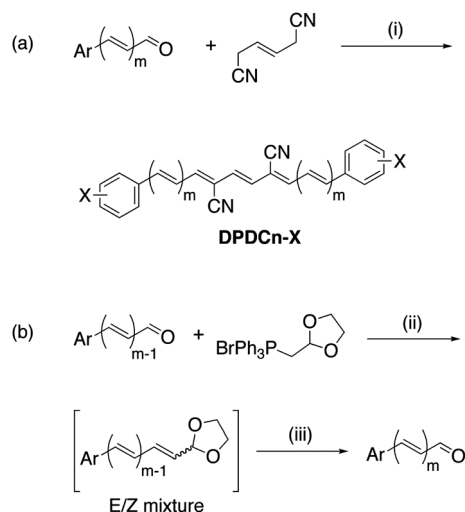
In order to use oligoenes in optical devices, it is desirable to have a family of light-harvesters that cover the entire visible and near-infrared spectral regions. Therefore, we sought small and synthetically available substituents that could confer stability while maintaining the bathochromic absorption shifts expected for longer oligoenes. Cyano groups fulfill these requirements: they are  $\pi$ -electron withdrawing groups that are not bulky enough to disrupt molecular planarity.<sup>13</sup> They have been used to alter the band gaps of aromatic molecules and conjugated polymer materials.<sup>14</sup> Because of their electron-withdrawing ability,<sup>15</sup> they are expected to lower the energies of the frontier orbitals, thus stabilizing the system toward oxidative decomposition. As an ultimate benefit they are easily installed and enable an economical synthesis that allows for diverse end-group functionalization.

## Results and discussion

### Synthesis

The nexus of our convergent synthesis of the oligoenes is the Knoevenagel condensation<sup>16</sup> between 1,4-dicyano-2-butene and two equivalents of the appropriate aryl-enal (Scheme 1a). We prepare the aryl-enals starting from the analogous benzaldehyde or *trans*-cinnamaldehyde *via* iterative Wittig homologations<sup>17</sup> and subsequent acidic hydrolysis of the intermediate acetal. The conditions for both reactions tolerate a wide variety of functionality and give access to a range of derivatives. Fig. 1 shows those derivatives that we prepared for this study *via* this method. They are made in a small number of steps from commercially available starting materials.

In general the Knoevenagel condensations give moderate yields, which decrease with increasing molecular length, producing the **DPDCn** series in 10–60% isolated yields as shown



**Scheme 1** Synthesis of DPDCs *via* (a) double-Knoevenagel condensation reaction and (b) Wittig reaction. *Reagents and conditions:* (i) DBU, MeOH, 25 °C, 6–12 h, (60–10% for **DPDCn** series; from  $m = 0$ –5); (ii) LiOMe, THF, 75 °C, 12–24 h; (iii) 10% aq. HCl, 25 °C, 2 h (70–98%). For instance, if  $m = 1$ , then the intermediate acetal leads to the product (*2E,4E*)-5-phenylpenta-2,4-dienal. A list of all compounds is provided in ESI†.

**Table 1** Double Knoevenagel condensation yields for the unfunctionalized **DPDCn** series

Oligoene	Oligomeric length ( <i>n</i> )	Isolated yield (%)
<b>DPDC3</b>	3	55
<b>DPDC5</b>	5	60
<b>DPDC7</b>	7	54
<b>DPDC9</b>	9	45
<b>DPDC11</b>	11	40
<b>DPDC13</b>	13	10

in Table 1. Nonetheless, the condensation reaction is operationally simple: it does not require anhydrous solvents and the isolation does not require chromatography. This reaction joins two fragments together and more than doubles the length of the oligomers. The products precipitate from the reaction mixture and are easily isolated by filtration. We purify the crude product by recrystallization from  $\text{CH}_2\text{Cl}_2$ –MeOH. With this approach, the synthesis of **DPDC13** (one of the longest oligoenes prepared to date) is straightforward and involves only five steps. It is also important to mention that the sequence shown in Scheme 1 is scalable; we tested some derivatives on the gram-scale with no loss in their isolated yields.

All of the compounds have exclusively *trans*-stereochemistry in their double bonds. The stereochemistry of the double bonds in the each aldehyde can be identified by the coupling constants of the olefinic doublet of doublets near 6.5 ppm (this signal belongs to the  $\beta$ -proton of the aryl-enal). This resonance is coupled to the protons of the terminal aldehyde and to a *trans*-olefin ( $-\text{CH}=\text{C}$ ) proton. This resonance resides in an isolated region of the spectra allowing for stereochemical characterization throughout the growth of the aryl-oligoenals. Wittig conditions (Scheme 1b) produce an *E/Z*-mixture of stereoisomers, however acidolysis of the intermediate acetals exclusively produces the *trans*-product. Cleavage of the acetal is carried out before separation; however, to further understand our method we tracked the stereoisomeric transformations throughout the extension of *trans*-cinnamaldehyde to (2*E*,4*E*)-5-phenylpenta-2,4-dienal. In this case performing the Wittig reaction on *trans*-cinnamaldehyde produces the (*E*)- and (*Z*)-4-phenylpenta-2,4-dienyl acetals in 16 and 60% yield, respectively. We separated each product by column chromatography; coupling constants from  $^1\text{H}$  NMR spectra identified each stereoisomer. Acid hydrolysis of either stereoisomer, *E* or *Z*, generates the same product, (2*E*,4*E*)-5-phenylpenta-2,4-dienal, in quantitative yields.

In order to verify the practical value of cyano substitution, we have also prepared the unsubstituted  $\alpha,\omega$ -diphenyl-oligoenes of the corresponding lengths. We synthesized these molecules lacking the cyano groups *via* the Horner–Wadsworth–Emmons reaction<sup>18</sup> as described by Spangler and co-workers.<sup>10</sup> Dicyano-oligoenes are much less reactive toward ambient oxidation, intermolecular oligomerization or intramolecular decomposition than their unsubstituted relatives and we can conveniently study them under normal aerobic laboratory conditions for extended periods.<sup>19</sup> The thermal stability of these dicyano-oligoenes (**DPDC3**–**DPDC13**) is similar to that of the  $\alpha,\alpha,\omega,\omega$ -tetrakis-*tert*-butyl-functionalized oligoenes reported by Hopf and

co-workers<sup>9</sup> and far higher than that of the methyl and unfunctionalized analogs.<sup>20</sup> Differential scanning calorimetry shows that under an inert atmosphere all members of the parent series **DPDC3**–**DPDC13** are thermally stable up to  $\sim 250$  °C. For a direct comparison between cyano-functionalized and unfunctionalized oligoenes, we photooxidatively decomposed both **DPO5** and **DPDC5** in a side-by-side experiment. We monitored the oligoene starting materials with UV-vis spectroscopy and found that the unsubstituted material decomposes four times faster than the cyano-functionalized material.<sup>21</sup>

### Band-gap modulation

In order to appraise the effects of cyano-substitution we first consider the derivatives that have unsubstituted phenyl groups, **DPDCn**. Despite providing stabilization to the oligoene core, the cyano groups do not fundamentally alter the “polyacetylene-like” electronic behavior of oligoenes in the sense that the HOMO–LUMO gap decreases as the length of the oligoene increases, which is typical of other vinylogous series.<sup>22</sup> The optical absorptions of the **DPDCn** series for *n* between 3 and 13 span the entire visible spectrum (Fig. 2a). The absorptions are also quite intense with molar extinction coefficients ( $\epsilon$ ) that exceed  $10^5$   $\text{M}^{-1} \text{cm}^{-1}$ . We estimate the solution-phase optical band gap ( $E_{\text{og}}$ ) for **DPDC11** and **DPDC13** to be 1.81 and 1.77 eV, respectively. These values approach the band gap observed for PA itself.<sup>23</sup> Similarly, we can analyze this series using the quantum mechanical “particle in a box” model, which is often used to describe optical absorptions in one-dimensional systems. This model holds that the excitation energies in a simple system vary with the inverse square of the dimensional length. Fitting the excitation energies in the **DPDCn** series with such an inverse-square expression (see Fig. 2c) leads to an effective mass of  $2.15 \times 10^{-45}$  kg. Extrapolation of the wavelength for the strongest absorption ( $\lambda_{\text{max}}$ ) and optical band gap ( $E_{\text{og}}$ ) to an infinite “box” length estimates values of 577 nm and 1.59 eV, respectively. This is within the reported range of band gaps (1.4–1.6 eV) for *trans*-PA.<sup>1,23</sup> Our extrapolations were carried out as simple linear regression analyses; the Meier correction<sup>24</sup> did not provide any benefit in this case because the effective conjugation length (ECL) had not been reached. The ECL of polyenes is higher than other poly-conjugated systems<sup>22</sup> and has been estimated to lie between 15 and 20 repeat units.<sup>4,25</sup> We estimate the ECL of a DPDC polymer by selecting the point in our three extrapolations where a change in oligomeric length of one repeat unit corresponds to a negligible energy difference of less than 0.01 eV. In each case, the emergence of size-independent electronic properties ( $\lambda_{\text{max}}$ ,  $E_{\text{og}}$  and  $E_{\text{cv}}$ ) is predicted to occur at lengths  $\geq 19$  alkene repeat units.

Since cyano groups are strongly electron withdrawing, their presence should lower the energies of the frontier orbitals with respect to those of the unfunctionalized  $\alpha,\omega$ -diphenyl-oligoenes. The redox potentials determined by cyclic voltammetry were used to estimate the energies of the HOMOs and LUMOs of the **DPDCn** series. We found that installation of two cyano groups onto the oligoene core stabilizes the HOMO and LUMO by as much as 0.44 and 0.68 eV with respect to the corresponding unsubstituted **DPOn** molecules (Fig. 2b). This is consistent with UV-vis absorption spectroscopy, in which we observe

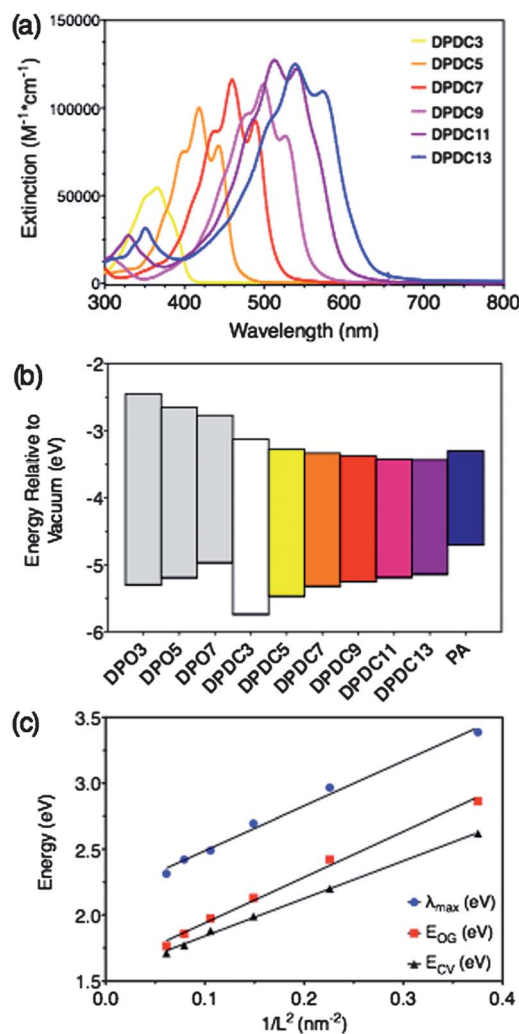


**Fig. 2** (a) UV-vis absorption spectra of the parent oligoene series (DPDCn) in CH<sub>2</sub>Cl<sub>2</sub>. Plot of extinction coefficient vs. absorption wavelength. The wavelength of strongest absorption,  $\lambda_{\max}$  (from left to right) at 363, 418, 459, 499, 513 and 536 nm; increasing the length of oligomers tunes the optical absorptions over a range of 350 nm. (b) Effect of the cyano groups on the HOMO and LUMO energies of diphenyl-oligoenes determined by cyclic voltammetry (CV). Redox gap of DPO3, DPO5, DPO7 (grey) and the cyano-functionalized series, DPDCn. CVs were obtained in DMF solution with 0.1 M (*n*-Bu)<sub>4</sub>N<sup>+</sup>PF<sub>6</sub><sup>-</sup>. Ferrocene was used as an internal standard for electrochemical measurements. Experimentally determined values for PA (blue) are included for reference.<sup>23</sup> (c)  $\lambda_{\max}$ , the optical band gap ( $E_{\text{og}}$ ) and the redox band gap ( $E_{\text{cv}}$ ) for the DPDCn series are fit using “particle in a box” energies. Extrapolative analysis estimates the analogous values for an oligomer of infinite length (polymer) of 577 nm, 1.59 eV and 1.55 eV, respectively. Predicted values agree with experimentally determined values for PA.

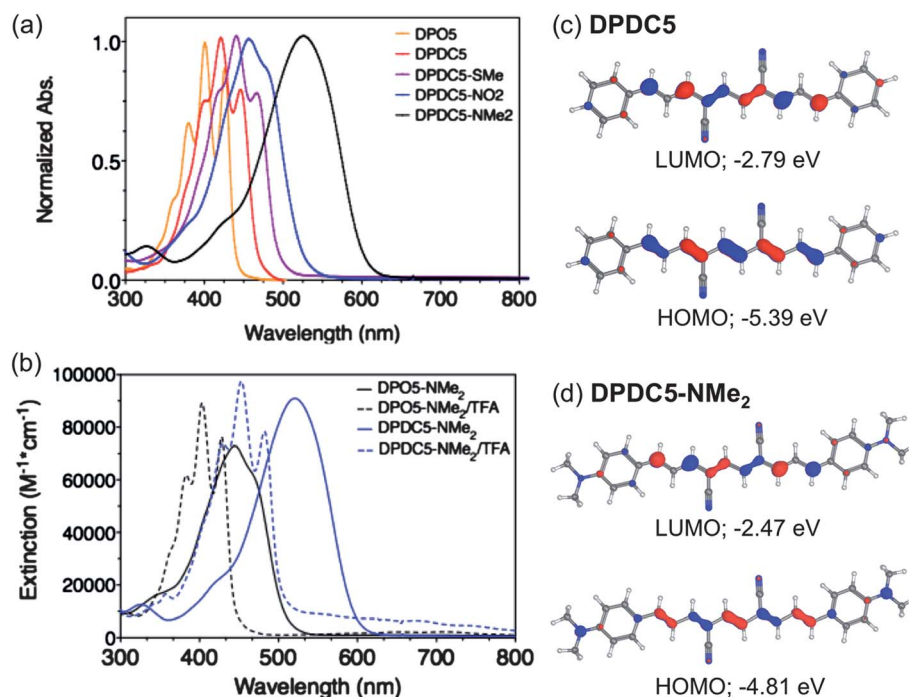
a bathochromic shift of up to 35 nm between the DPOn and DPDCn series (see Fig. 3a). The electrochemically determined energy gap,  $E_{\text{cv}}$ , for DPDCn molecules can also be extrapolated to predict the band gap of the homologous polymer. In Fig. 2c we again use simple “particle in a box” energies to predict the band gap for the polymer to be 1.55 eV. Both the  $E_{\text{cv}}$  and the  $E_{\text{og}}$  converge to similar values.

## End-functionalized derivatives

Substitution on the terminal phenyl groups offers another opportunity to tailor the electrical and physical properties of oligoenes. We synthesized a family of derivatives of DPDC5 (Table 2), whose phenyl-substituents varied from strongly electron-withdrawing (NO<sub>2</sub>) to electron-donating (NMe<sub>2</sub>). We found *para*-substitution to be most effective, apparently since it is strongly resonance-coupled to the oligoene backbone and at the same time sterically remote (see Fig. S4, ESI†). Spangler and co-workers reported similar results for non-cyano DPOs having *para*-substituents NO<sub>2</sub>, Cl, SMe, OMe and NMe<sub>2</sub>.<sup>10</sup> Examples of the effect of aryl-functionalization on the optical absorption are displayed in Fig. 3a. Strong electron-donating groups give the largest bathochromic shifts and broadened absorption peaks. Functionalization of the DPDC5 scaffold with *p*-NMe<sub>2</sub> groups shifts the longest-wavelength absorption from 490 to 640 nm, and this shift is accompanied by the loss of vibronic fine-structure.<sup>26</sup> These electronic differences indicate topological changes in the frontier orbitals due to a transformation from an oligoene  $\pi$ - $\pi^*$  excitation to a “push-pull”  $n$ - $\pi^*$  transition; giving rise to an intramolecular charge transfer (ICT).<sup>27</sup> We performed time-dependent density functional theory (TD-DFT)<sup>28</sup> calculations at the B3LYP/6-31\*\* level on DPDC5 and DPDC5-NMe<sub>2</sub> to investigate their excited states and the topologies of relevant molecular orbitals. In each case we found that the lowest-energy excitation is predominantly promotion of an electron from the HOMO to the LUMO, and in each case this transition is strongly allowed. We show these frontier orbitals for each molecule in Fig. 3c and d, respectively. The LUMOs of DPDC5 and DPDC5-NMe<sub>2</sub> are remarkably similar: each is primarily the expected, lowest-energy  $\pi^*$ -orbital of a conjugated polyene. However, the HOMOs of the two molecules differ. While the HOMO of DPDC5 is primarily the expected, highest-energy  $\pi$ -orbital of the polyene, in DPDC5-NMe<sub>2</sub> there is significant electron density on the terminal aryl groups and the nitrogen lone pairs. A similar trend in the frontier orbitals is predicted even when the cyano groups are removed from the oligoene core (see Fig. S14, ESI†) implying that the cyano groups contribute less to the intramolecular charge transfer (ICT) than do the NMe<sub>2</sub> groups. Thus while the HOMO–LUMO excitation in DPDC5 is largely  $\pi$ - $\pi^*$ , that in DPDC5-NMe<sub>2</sub> has a significant component of  $n$ - $\pi^*$  character. This may be considered ICT.<sup>29</sup>

Since the HOMO–LUMO transition in DPDC5-NMe<sub>2</sub> is due, at least in part, to  $n$ - $\pi^*$  promotion, protonation of the nitrogens should remove the nitrogen lone pair participation in the HOMO and therefore quench any ICT, leaving behind the  $\pi$ - $\pi^*$  absorptions of the oligoene. Indeed, addition of trifluoroacetic acid to solutions of DPDC5-NMe<sub>2</sub> and DPO5-NMe<sub>2</sub> resulted in a hypsochromic shift and resolution of the vibronic fine-structure as seen in Fig. 3b. The effect is reversible; when we neutralize the erstwhile acidic solutions with triethylamine, absorption is again shifted to the red and the vibronic structure is lost.

Solvatochromism may be used to assess the amount of ICT behavior in conjugated push-pull systems, since the polarizability of  $\pi$ -electrons partially depends on the environment provided by the solvent, such as polarizability and solvent cavity size.<sup>29</sup> The absorption behavior of DPDC5-NMe<sub>2</sub> was surveyed throughout 15 organic solvents. The value of  $\lambda_{\max}$  was observed

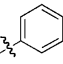
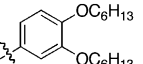
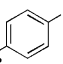
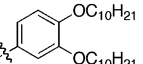
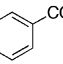
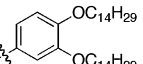
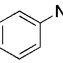
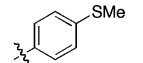
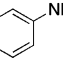
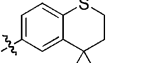


**Fig. 3** (a) UV-vis absorption spectra of oligoene derivatives in CH<sub>2</sub>Cl<sub>2</sub>; DPO5 (orange), DPDC5 (red), DPDC5-SMe (purple), DPDC5-NO<sub>2</sub> (blue) and DPDC5-NMe<sub>2</sub> (black). For easy comparison absorptions have been normalized to 1. (b) Absorption spectra of protonated (solid line) and deprotonated (dashed line) forms of DPDC5-NMe<sub>2</sub> (black) and DPO5-NMe<sub>2</sub> (blue) in CH<sub>2</sub>Cl<sub>2</sub>. TD-DFT calculations compare the LUMO and HOMO of (c) DPDC5 and (d) DPDC5-NMe<sub>2</sub>.

to shift 55 nm from solutions of heptane to nitrobenzene, while the longest-wavelength absorption shifted 70 nm from heptane to dimethyl sulfoxide (DMSO) (see Fig. S7, ESI†).

The rigid structure of conjugated oligoenes leaves them sparingly soluble in organic solvents and hinders solution-based processing techniques such as spin-casting or inkjet printing.

**Table 2** Comparison of selected DPDC5 derivatives and their UV-vis strongest-wavelength absorptions in CH<sub>2</sub>Cl<sub>2</sub> solution

Entry	R	$\lambda_{\max}^a/nm$ (eV)	Entry	R	$\lambda_{\max}^a/nm$ (eV)
1		418 (2.97)	6		454 (2.73)
	<b>DPDC5</b>			<b>DPDC5-OC<sub>8</sub>H<sub>13</sub></b>	
2		426 (2.91)	7		454 (2.73)
	<b>DPDC5-Br</b>			<b>DPDC5-OC<sub>10</sub>H<sub>21</sub></b>	
3		434 <sup>b</sup> (2.86)	8		455 (2.73)
	<b>DPDC5-CO<sub>2</sub>H</b>			<b>DPDC5-OC<sub>14</sub>H<sub>29</sub></b>	
4		437 (2.84)	9		453 (2.74)
	<b>DPDC5-NO<sub>2</sub></b>			<b>DPDC5-SMe</b>	
5		521 (2.38)	10		463 (2.68)
	<b>DPDC5-NMe<sub>2</sub></b>			<b>DPDC5-SC<sub>5</sub>H<sub>10</sub></b>	

<sup>a</sup> Strongest wavelength absorption is taken at the global  $\lambda_{\max}$  and is not indicative of HOMO–LUMO gap energies,  $E_{\text{og}}$ . <sup>b</sup> Due to the limited solubility absorption spectrum was taken in DMSO.

This is an important obstacle for promising organic electronic materials to overcome for application in film-based technologies. Again, we take advantage of the facile functionalization of phenyl end-groups in order to enhance oligoene solubility. Long alkoxy groups and bulky thioethers (Table 2, entries 6–10) tune the solubility over a wide range while maintaining consonant electronic properties (based on UV-vis absorption, as well as  $^1\text{H}$  and  $^{13}\text{C}$ NMR spectra; see Fig. S5, ESI†). For example, **DPDC5-OC<sub>14</sub>H<sub>29</sub>** and **DPDC5-SC<sub>5</sub>H<sub>10</sub>** reach molarities up to  $\sim 0.10$  M in chloroform at room temperature; increasing the solubility from  $\sim 10^{-4}$  M for **DPDC5**. These derivatives are also soluble in other common organic solvents such as toluene, tetrahydrofuran and benzene. Using this synthetic approach, longer alkoxy chains or even polymeric attachments are presumed to be possible.

### Solid-state structures

We have grown crystals of each member of the **DPDC<sub>n</sub>** family (from  $n = 3$  to 13) and determined the molecular structure of each crystallographically. Each oligoene occurs exclusively in the all-*trans* form. **DPDC13** (Fig. 4) is the longest oligoene thus far characterized by XRD, longer even than the natural product, rhodopin glucoside,<sup>30</sup> which contains 11 linear conjugated C=C bonds. Although some of the shorter vinylogues have been previously reported in the resin dye patent literature,<sup>31</sup> a systematic characterization has been heretofore unavailable. Only a few non-terpenoid structures having more than six conjugated C=C bonds have been previously reported, and none having more than nine.<sup>32</sup>

We observe different packing structures within the parent series of **DPDC<sub>n</sub>** oligomers. The shortest vinylogues, **DPDC3** and **DPDC5**, are planar and stack in a herringbone pattern, indicating that the cyano groups do not significantly interact with allylic hydrogens (see Fig. S10, ESI†). The longer oligomers, **DPDC7–DPDC13**, co-crystallize with one solvent molecule per unit cell and are not fully planar. The central dicyanobutene moiety is planar and to either side out-of-plane bending of the conjugated backbone is accompanied by a slight twist. DFT calculations at the B3LYP/6-31G\*\* level predict fully planar conformations, however the incorporation of solvent as well as

bending is common in crystal structures of oligoenes having more than six C=C bonds.<sup>8,9,32</sup>

We were concerned that the cyano groups would disturb the local structure of the oligoene backbone and minimize the degree of conjugation. Despite the observed bending, the central alkene unit (that having doubly allylic cyano groups) remains planar with a dihedral angle of  $180.0^\circ$ . This suggests that deviations from planarity may be attributed to co-crystallization with solvent molecules and not the result of cyano-functionalization.

The molecular organization in the solid state changes when we functionalize the DPDCs with carboxylate groups. Unlike the pentaene of the parent series (**DPDC5**), crystals of **DPDC5-CO<sub>2</sub>H** contain two molecules of solvent, dimethylformamide (DMF), per oligoene and do not organize in a herringbone structure. In Fig. 5 we show that hydrogen bonding with DMF facilitates the assembly of the carboxylic acids into  $\pi$ -stacked sheets of oligoenes. The lack of solvent between oligoenes allows for the intermolecular distances to decrease to 3.38 Å between  $\pi$ -faces of neighboring molecules. These values approach the interplanar distances found for the classic carbon allotrope, graphite; 3.35 Å.<sup>33</sup> **DPDC5-CO<sub>2</sub>H** stacks in an oblique alignment with six close neighbors oriented in a hexagonal pattern when viewed down the length of the molecule.<sup>34</sup> All molecules in the crystal are aligned in the same direction and overlap with neighboring molecules through  $\pi$ -stacking interactions. This is an ideal geometry for charge transport through a single crystal.

### Self-assembly

As a demonstration of how this synthetic control enables us to incorporate our molecular wires into materials, we used functionalized oligoenes, **DPDC3-CO<sub>2</sub>H**, to assemble monolayers of magnetic nanoparticles on GaAs substrates. It has been shown previously that carboxylic acids bind to GaAs<sup>35</sup> and Fe<sub>3</sub>O<sub>4</sub> through known ligand-exchange procedures.<sup>36</sup> First, the native oxide layer of the GaAs substrates were removed through submersion in aqueous ammonia (NH<sub>3</sub> aq). After rinsing with ethanol they were submerged in a 1.5 mM solution of oligoene (**DPDC3-CO<sub>2</sub>H**) in DMSO. They were then removed from solution, again rinsed with ethanol, and submerged for 1 h in a solution of 10-nm Fe<sub>3</sub>O<sub>4</sub> nanoparticles in DMF. Scanning

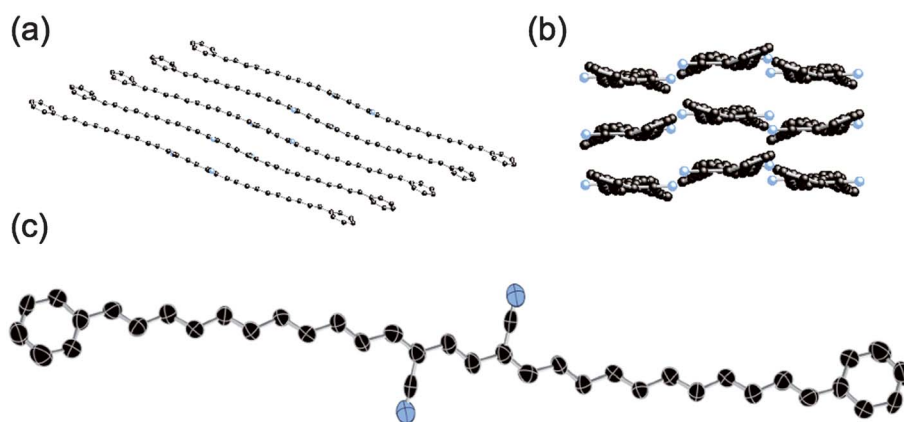


**Fig. 4** Packing structure of **DPDC13** (a) viewed from the side and (b) down the length of oligoene chain shows deviations from planarity. (c) ORTEP plot of **DPDC13**. Ellipsoids represent 50% probability levels. Hydrogen atoms have been omitted.

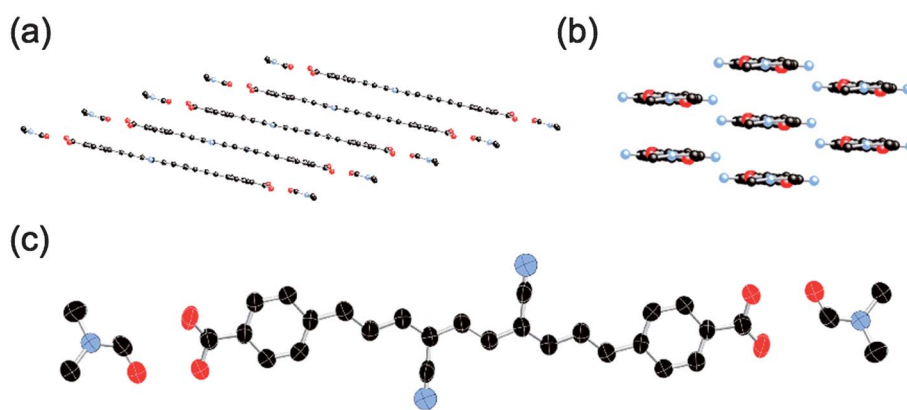


**Fig. 5** Packing structure of DPDC5-CO<sub>2</sub>H·2DMF (a) viewed from the side and (b) down the length of oligoene chain. (c) Ellipsoids represent 50% probability levels. Hydrogen atoms have been omitted.

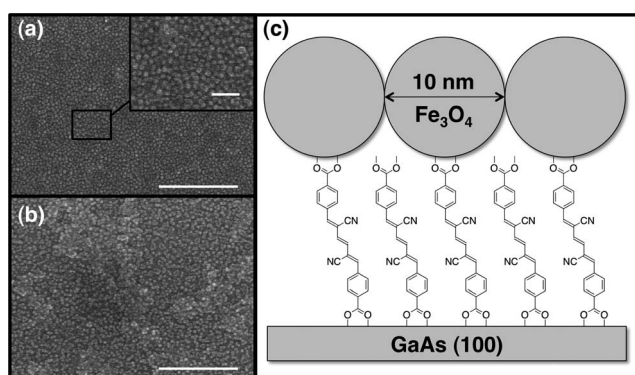


**Fig. 6** Scanning electron micrographs (SEM) of 10-nm Fe<sub>3</sub>O<sub>4</sub> nanoparticle SAMs made using (a) 1.5 mM and (b) 3.0 mM solution of DPDC3-CO<sub>2</sub>H, show monolayer coverage at low concentrations and the presence of multilayers at higher concentration. Scale bars are set to 500 nm, while the inset scale bar is set to 50 nm. (c) Schematic of oligoene-Fe<sub>3</sub>O<sub>4</sub> composite monolayer.

electron microscopy (SEM) analysis of these films shows clear formation of nanoparticle monolayers as shown in Fig. 6. Nanoparticle coverage was found to be dependent upon the concentration (1.5, 3.0 or 6.0 mM) of the oligoene solution. At higher concentrations (3.0 and 6.0 mM) the appearance of multilayers in addition to monolayers was observed (Fig. 6b; Fig. S12, ESI†). No monolayer formation was observed when only DMSO without oligoene was used or upon the direct submersion of the GaAs substrate into the nanoparticle solution (see Fig. S12, ESI†).

## Conclusion

We have developed a new method to synthesize cyano-substituted oligoenes with up to 13 all-*trans* conjugated C=C bonds, and we have demonstrated its utility in the synthesis of a wide variety of aryl-functionalized oligoenes. Cyano groups decrease the band gap of oligoenes and stabilize them for study under normal laboratory conditions while preserving the conjugation along the poly-olefin backbone. Derivatization of the terminal phenyl groups allows us to fine tune the electronic structure and physical properties. We can access practically any

energy within the visible spectral region by pairing the appropriate oligoene length with the appropriate aryl end-group. Functionalized oligoenes are ideal structures for nanoscale electronic and structural components and can be used to guide oligoene self-assembly and the construction of heterogeneous materials. Furthermore, the utility of these materials in photovoltaics is an obvious application since their band gaps are easily tuned, their absorptions cover the visible spectrum, and they are predicted to be useful in singlet fission.<sup>37</sup>

## Acknowledgements

The authors would like to acknowledge Hanfei Wang, Hasti Amiri and Alon Gorodetsky for their technical assistance with SEM and electrochemistry. Authors also thank the Prof. Gerard Parkin for XRD expertise.

## Notes and references

- (a) C. K. Chiang, M. A. Drury, S. C. Gau, A. J. Heeger, E. J. Louis, A. G. MacDiarmid, Y. W. Park and H. Shiraka, *J. Am. Chem. Soc.*, 1978, **100**, 1013–1015; (b) Y. W. Park, A. J. Heeger, M. A. Drury and A. G. MacDiarmid, *J. Chem. Phys.*, 1980, **73**, 946–957.
- (a) F. Kajzar, S. Etemad, G. L. Baker and J. Messier, *Solid State Commun.*, 1987, **63**, 1113–1117; (b) W. S. Fann, S. Benson, J. M. J. Madey, S. Etemad, G. L. Baker and F. Kajzar, *Phys. Rev. Lett.*, 1989, **62**, 1492–1495.
- (a) R. R. Burch, Y. Dong, C. Fincher, M. Goldfinger and P. E. Rouviere, *Synth. Met.*, 2004, **146**, 43–46; (b) J. He, F. Chen, J. Li, O. F. Sankey, Y. Terazono, C. Herrero, D. Gust, T. A. Moore, A. L. Moore and S. M. Lindsay, *J. Am. Chem. Soc.*, 2005, **127**, 1384–1385; (c) I. Visoly-Fisher, K. Daie, Y. Terazono, C. Herrero, F. Fungo, L. Otero, E. Durantini, J. J. Silber, L. Sereno, D. Gust, T. A. Moore, L. A. Moore and S. M. Lindsay, *Proc. Natl. Acad. Sci. U. S. A.*, 2006, **103**, 8686–8690.
- (a) K. Knoll, K. A. Krouse and R. R. Schrock, *J. Am. Chem. Soc.*, 1988, **110**, 4424–4425; (b) K. Knoll and R. R. Schrock, *J. Am. Chem. Soc.*, 1989, **111**, 7989–8004; (c) C. Scriban, B. S. Amagai, E. A. Stemmler, R. L. Christensen and R. R. Schrock, *J. Am. Chem. Soc.*, 2009, **131**, 13441–13452.
- The symbols,  $\mu$  and  $\nu$ , are used to designate central positions along the oligoene main chain, because they are the middle letters in the Greek alphabet. This nomenclature is unprecedented, but serves to distinguish central locations from the terminal locations,  $\alpha$  and  $\omega$ .
- R. Kuhn, *Angew. Chem.*, 1937, **50**, 703–718.
- J. S. Meisner, M. Kamanetska, M. Krikorian, M. Steigerwald, L. Venkataraman and C. Nuckolls, *Nano Lett.*, 2011, **11**, 1575–1579.

- 8 A. Kiehl, A. Eberhardt and K. Müllen, *Liebigs Ann. Chem.*, 1995, 223–230.
- 9 D. Klein, P. Kiliçkiran, C. Mlynek, H. Hopf, I. Dix and P. G. Jones, *Chem.–Eur. J.*, 2010, **16**, 10507–10522.
- 10 (a) C. W. Spangler, R. K. McCoy, A. A. Dembek, L. S. Sapochak and B. D. Gates, *J. Chem. Soc., Perkin Trans. 1*, 1989, 151–154; (b) C. W. Spangler, P. K. Liu, A. A. Dembek and K. Havelka, *J. Chem. Soc., Perkin Trans. 1*, 1991, 799–802.
- 11 (a) L. Duhatuel and P. Duhamel, *Tetrahedron Lett.*, 1993, **34**, 7399–7400; (b) W. Froehlich, H. J. Dewey, H. Deger, B. Dick, K. A. Klingensmith, W. Puettmann, E. Vogel, G. Hohlneicher and J. Michl, *J. Am. Chem. Soc.*, 1983, **105**, 6211–6220.
- 12 (a) H. Nakamichi and T. Okada, *Angew. Chem., Int. Ed.*, 2006, **45**, 4270–4273; (b) G. Duester, *Cell*, 2008, **134**, 921–931; (c) T. Polívka and H. A. Frank, *Acc. Chem. Res.*, 2010, **43**, 1125–1134; (d) for general carotenoid reference, see: H. A. Frank, G. Britton, A. J. Young, A. Young and R. J. Cogdell, in *The Photochemistry of Carotenoids*, Springer-Verlag, New York, 2000.
- 13 An *A*-value of cyano groups has been determined to be 0.19 kcal mol<sup>-1</sup> in contrast to that of a methyl group (1.74 kcal mol<sup>-1</sup>). See: (a) H. J. Schneider and V. Hoppen, *J. Org. Chem.*, 1978, **43**, 3866–3873; (b) H. Booth and J. R. Everette, *J. Chem. Soc., Chem. Commun.*, 1976, 278–279.
- 14 (a) O. W. Webster, *J. Polym. Sci., Part A: Polym. Chem.*, 2002, **40**, 210–221; (b) M. S. Liu, X. Jiang, S. Liu, P. Herguth and A. K.-Y. Jen, *Macromolecules*, 2002, **35**, 3532–3538; (c) Y.-F. Lim, Y. Shu, S. R. Parkin, J. E. Anthony and G. G. Malliaras, *J. Mater. Chem.*, 2009, **19**, 3049; (d) M. L. Kaplan, R. C. Haddon, F. B. Bramwell, F. Wudl, J. H. Marshall, D. O. Cowan and S. Gronowitz, *J. Phys. Chem.*, 1980, **84**, 427–431; (e) M. J. Ahrens, M. J. Fuller and M. R. Wasielewski, *Chem. Mater.*, 2003, **15**, 2684–2686.
- 15 Cyano groups are known as strong electron-withdrawing groups as evidenced by their high Hammett substituent coefficient ( $\sigma_p = 0.66$ ). See: C. Hansch, A. Leo and R. W. Taft, *Chem. Rev.*, 1991, **91**, 165–195.
- 16 E. Knoevenagel, *Ber. Dtsch. Chem. Ges.*, 1898, **31**, 2596–2619.
- 17 (a) G. Wittig and U. Schoellkopf, *Chem. Ber.*, 1954, **87**, 1318–1330; (b) G. Wittig and W. Haag, *Chem. Ber.*, 1955, **88**, 1654–1666.
- 18 W. S. Wadsworth, *Org. React.*, 1977, **25**, 73.
- 19 Stability of **DPDCn** series was observed by <sup>1</sup>H NMR and thin layer chromatography over the duration of six months. When stored at 0 °C in the absence of light **DPDCn** and **DPOn** series showed no signs of degradation. When stored on the bench top in ambient conditions **DPDC3–DPDC7** also did not degrade. However, the degradation of **DPDC9–DPDC13** were observed and increased with increased molecular length. Broadened peaks were found in their <sup>1</sup>H NMR spectra and **DPDC13** was observed to lighten in color. At short lengths ( $n = 3–7$ ) **DPDCn** and **DPOn** series are stable in ambient conditions. Further comparisons between the each series were limited, since we were unable to synthesize/characterize longer **DPOn** molecules due to very low solubility.
- 20 (a) F. Bohlmann and H. J. Mannhardt, *Chem. Ber.*, 1956, **89**, 1307–1315; (b) P. Nayler and M. C. Whiting, *J. Chem. Soc.*, 1955, 3037–3047; (c) F. Sondheimer, D. A. Ben-Efraim and R. Wolovsky, *J. Am. Chem. Soc.*, 1961, **83**, 1675–1681; (d) F. Sondheimer, D. A. Ben-Efraim and Y. Gaoni, *J. Am. Chem. Soc.*, 1961, **83**, 1682–1685.
- 21 Dilute solutions ( $\sim 10^{-4}$  M) of **DPO5** and **DPDC5** were prepared and irradiated with a 450 W ACE mercury lamp (#7825–34) at room temperature. This procedure was carried out under both aerobic and anaerobic conditions. We observed degradation of **DPO5** and **DPDC5** through the loss of their longest-wavelength absorbance by UV-vis spectrometry.
- 22 Y. Geerts, G. Klaerner, K. Muellen, in *Electronic materials: The Oligomeric Approach*, ed. K. Muellen and G. Wegner, Wiley-VHC, New York, 1998, pp. 3–25, 360 and 406–410, and references therein.
- 23 Reported experimental values for PA cover a wide range owing to different methods of polymer and film preparation. See the following and references therein: (a) H. Fujimoto, K. Kamiya and J. Tanaka, *Synth. Met.*, 1985, **10**, 367–375; (b) K. A. O. Starzewki and G. M. Bayer, *Angew. Chem., Int. Ed. Engl.*, 1991, **30**, 961–962; (c) F. Krausz, P. Lásztity and J. S. Bakos, *Appl. Phys. B: Photophys. Laser Chem.*, 1988, **45**, 21–25.
- 24 H. Meier, U. Stalmach and H. Kolshorn, *Acta Polym.*, 1997, **48**, 379–384.
- 25 (a) M. Rumi, A. Kiehl and G. Zerbi, *Chem. Phys. Lett.*, 1994, **231**, 70–74; (b) V. Hernandez, C. Castiglioni, M. Del Zoppo and G. Zerbi, *Phys. Rev. B: Condens. Matter*, 1994, **50**, 9815; (c) J. L. Brédas, R. Silbey, D. S. Boudreeaux and R. R. Chance, *J. Am. Chem. Soc.*, 1983, **105**, 6555–6559.
- 26 (a) B. E. Kohler, *J. Chem. Phys.*, 1988, **88**, 2788–2792; (b) B. E. Kohler, C. Spangler and C. Westerfield, *J. Chem. Phys.*, 1988, **89**, 5422–5428.
- 27 (a) B. Breiten, Y.-L. Wu, P. D. Jarowski, J.-P. Gisselbrecht, C. Boudon, M. Griesser, C. Onitsch, G. Gescheidt, W. B. Schweizer, N. Langer, C. Lennartz and F. Diederich, *Chem. Sci.*, 2011, **2**, 88; (b) L.-O. Pålsson, C. Wang, A. S. Batsanov, S. M. King, A. Beeby, A. P. Monkman and M. R. Bryce, *Chem.–Eur. J.*, 2010, **16**, 1470–1479.
- 28 DFT calculations were run using *Jaguar version 7.7*, Schrodinger LLC, New York, 2010.
- 29 (a) F. Bures, O. Pytela and F. Diederich, *J. Phys. Org. Chem.*, 2011, **24**, 274–281; (b) F. Bovey and S. Yanari, *Nature*, 1960, **186**, 1042–1044.
- 30 G. McDermott, S. M. Prince, A. A. Freer, A. M. Hawthornthwaite-Lawless, M. Z. Papiz, R. J. Cogdell and N. W. Isaacs, *Nature*, 1995, **374**, 517–521.
- 31 (a) J. G. J. Kok, R. Van Moorselaar and A. Noordermeer, Verfahren zum Faerben synthetischer Harze und gefaerbte Harze, *Ger. Pat.*, DE 2230783, June 23, 1972; (b) C. M. Langkammerer, Reaction products of 3-hexenedinitrile and certain aldehydes, *US Pat.*, US 2462407, February 22, 1949.
- 32 There exists a dearth of solid-state structural information on oligoenes especially for those having more than five linear conjugated C=C bonds. For instance, the Cambridge Structural Database (CSD) provides only two non-terpenoid (such as carotenoids) oligoene structures containing nine linear conjugated C=C double bonds. Both structures belong to the cyclic oligomer, [18]-annulene (see: S. Gorter, E. Rutten-Keulemans, M. Krever, C. Romers and D. W. J. Cruickshank, *Acta Crystallogr., Sect. B: Struct. Sci.*, 1995, **51**, 1036–1045). Other search results show 6 structures for  $n = 8$ , 10 for  $n = 7$ , and 13 for  $n = 6$ .
- 33 Y. Baskin and L. Meyer, *Phys. Rev.*, 1955, **100**, 544.
- 34 The oblique packing structures of **DPDC7–DPDC13** and **DPDC5–CO<sub>2</sub>H** differ from the herringbone-type structure found in polyacetylene, which more closely resemble structures for **DPDC3** and **DPDC5**. See: C. R. Fincher, C.-E. Chen, A. J. Heeger, A. G. MacDiarmid and J. B. Hastings, *Phys. Rev. Lett.*, 1982, **48**, 100–104. The closest oligomeric approximation of the structure of polyacetylene can be made with *trans*-1,3,5,7-octatetraene, see: R. H. Baughman, B. E. Kohler, I. J. Levy and C. Spangler, *Synth. Met.*, 1985, **11**, 37–52.
- 35 J. Martz, L. Zuppiroli and F. Nüesch, *Langmuir*, 2004, **20**, 11428–11432.
- 36 A. Dong, X. Ye, J. Chen, Y. Kang, T. Gordon, J. M. Kikkawa and C. B. Murray, *J. Am. Chem. Soc.*, 2011, **133**, 998–1006.
- 37 B. M. Smith and J. Michl, *Chem. Rev.*, 2010, **110**, 6891–6936.